Bull. Chem. Soc. Ethiop. **2022**, 36(4), 923-934.
DOI: https://dx.doi.org/10.4314/bcse.v36i4.17

ISSN 1011-3924
Printed in Ethiopia
Online ISSN 1726-801X

A STUDY ON THE DEVELOPMENT OF SCAFFOLD FABRICATION USING CITRIC ACID POLYESTER - NANOHYDROXYAPATITE COMPOSITE

R. Indira[1*], V. Jaisankar[2] and S.C. Vella Durai[3]

[1]PG Department of Chemistry, Shrimathi Devkunvar Nanalal Bhatt Vaishnav College for Women, Chennai, Tamil Nadu, India
[2]Department of Chemistry, Presidency College, Chennai, Tamil Nadu, India
[3]Manonmaniam Sundaranar University College, Tirunelveli, Tamil Nadu, India

(Received March 8, 2022; Revised May 10, 2022; Accepted June 13, 2022)

ABSTRACT. Nano hydroxyapatite (n-HAp) and its composites have shown a great development in the field of tissue regeneration and in controlled drug delivery due to its good biocompatibility and bioactivity behavior. Furthermore, HAp-based nanocomposites enhance mechanical properties. These synthetic HAp nanocomposites can also be tailored to fabricate scaffold with controlled porosity which facilitate the growth of the cell in the field of tissue engineering. In this paper, we focus on the synthesis of nano hydroxyapatite (n-HAp) by sol-gel method. The synthesized nano powders were calcined at 500 ºC and characterized by FT-IR, XRD and TEM. We have also described the synthesis of citric acid-based polyester by melt polycondensation method without adding catalyst. The monomers used were citric acid, 1,6-hexane diol and sebacic acid. The corresponding synthesized n-HAp/polyester composite have potential application in soft tissue engineering. The structures of polyester and its nanocomposite were studied by FT-IR and ^{1}H NMR spectral studies. The thermal and mechanical properties of polyester, composites and cytotoxicity activity (MTT assay) using vero cells were also studied. Porous scaffold of the nano HAp/Polyester was fabricated by solvent-casting particulate leaching technique which is useful in the development of tissue engineering applications. SEM and TEM studies were carried out for nano HAp, polyester, composites and scaffold.

KEY WORDS: Cytotoxicity, Polycondensation, Sol-gel, Solvent-casting, Tissue engineering

INTRODUCTION

For the past few decades, synthetic biodegradable elastomers dominate in the field of tissue engineering, drug delivery system and gene treatment. Biodegradable elastomers were synthesized by melt polycondensation method but without adding catalyst which possesses suitable mechanical properties, suitable surface characteristics and bio-compatibility for fabrication of tissue engineering scaffolds [1]. Furthermore, there is increase in biocompatibility, mechanical strength and specific area of scaffolds with porosity can be prepared from nanocomposites. To fulfil the transplant conditions of fabricating scaffolds, biodegradable polyesters have chosen to be the most important biomaterial due to better biological activity and mechanical properties. Hence, we can improve the potential applications in bone tissue engineering [2]. Hydroxyapatite (HAp) has excellent biocompatible property and can be used in many biomedical applications such as bone substitutes, including prosthesis coatings, dental treatment, and as matrices for controlling drug delivery. Even in non-biomedical field HAp showed remarkable applications such as packing media for column chromatography, gas sensors, catalysis and as host materials for lasers [3, 4].

The mineral phase in human bone and HAp has similar chemical structure and shows a better affinity to host hard tissues [5, 6]. The main disadvantage of HAp is due to its poor mechanical properties which lead to formation of micro cracks during synthesis [7-9]. And also at high temperature, it can cause changes in Ca:P ratio. In order to improve its properties, the recent work

*Corresponding author. E-mail: induchem1985@gmail.com

in bio ceramics is mainly concentrated on improving their mechanical and biological properties by combining with biodegradable polyesters with HAp [10]. Many methods followed for synthesis of nano hydroxyapatite particles (n-HAp) have been reported such as precipitation [11], hydrothermal [12], hydrolysis [13], mechanochemical [14] and sol–gel [15]. Among the above methods, sol–gel method [15] is chosen to be the suitable method as it has the good uniform mixing of the calcium and phosphorus precursors, which improves chemical homogeneity of the resulting HAp to a significant extent, when compared to the traditional method. Furthermore, the reaction involves in sol-gel method does not need high temperature which decreases the calcinations temperature [16]. NaCl is chosen as porogen as it is convenient, less expensive and it can easily create pores while fabricating scaffolds. In this article, we report the novel synthesis and characterization of citric acid based polyester and the corresponding nanocomposite using HAp nano particles synthesized by sol-gel method and scaffold fabrication by particulate-leaching process.

EXPERIMENTAL

Materials

Sebacic acid (SeA) (99%) (Merck AR grade), 1, 6-hexane diol (HD) (99%) (Lancaster AR grade), and citric acid (CA) (99%) (Lancaster AR grade), were purchased and used as such. Sol-gel method was followed to prepare nano sized hydroxyapatite particles [17]. Minimal essential media (MEM) reagent, fetal bovine serum (FBS) and methylthiazolyl diphenyltetrazolium bromide (MTT) was used for cytotoxicity test. Porogen such as sodium chloride was used for fabrication of scaffold.

Synthesis of polyester

CA, HD and SeA were taken in the ratio 1:1:1, respectively. Initially the reaction mixture was melted at 160-165 ^{o}C and further the temperature was reduced to 140-145 ^{o}C. The stirring was continued for an hour which produces poly(1,6-hexanediol-sebacate-citrate), PHSeC pre-polymer. The pre-polyester can be cast into thin film by pouring the reaction mixture into Teflon Petri dish and kept in an oven at 90 ^{o}C for one week to get thin film of post polyesters.

Synthesis of nano-hydroxyapatite (n-HAp) by sol-gel method

The first step of synthesis of n-HAp involves the addition of prepared 0.25 M phosphoric acid with ammonia solution. Next, 1 M calcium nitrate tetra hydrate solution was added to the above mixture. In order to maintain pH = 10, drops of ammonia was added. Then the solution mixture was continuously stirred for an hour and kept for 24 hours undisturbed. A white color gel obtained was dried in an oven for 30 min. The temperature used for calcination is at 500 ^{o}C [18]. At this higher temperature, the hydroxy apatite gel attains the dried form. Finally, the dried gel was ground and sieved to get hydroxy apatite in nano sized particles.

Preparation of nano-hydroxy apatite/polymer composite

The synthesized polymers PHSeC was made to dissolve in ethanol with 1:1 w/v and mixed with 15% nano hydroxy apatite powder [19] and constantly stirred and poured into Teflon Petri dish and kept in an oven at 120 ^{o}C to get polymer nanocomposite thin film.

Preparation of scaffold using poly(1,6-hexanediol-sebacate-citrate)/nano hydroxyapatite composite

Yang *et al.* already worked with the same method for fabrication of scaffold using polyesters [1]. The porogen NaCl crystals were mixed with the PHSeC/n-HAp(15%)-dioxane mixture in the ratio

9:1, respectively and stirred vigorously for 24 hours and poured into Teflon Petri dish and kept in an oven at 110 ºC for a week. A thick spongy scaffold was obtained after curing process. Distilled water is poured into the scaffold and kept for 4 days to leach out the salt present in it. Preparation of porous scaffolds has been successfully processed by using a solvent-casting particulate leaching technique [20]. After four days, scaffold was taken out and freeze dried for further characterizations.

Cytotoxicity test (MTT assay)

Cytotoxicity test was carried out using vero cells with 1×10^5/well. The cells were incubated in 24-well plates at 37 ºC maintaining with 5% CO_2 condition. When the cell attains unification, the composite thin film was added and again kept for incubation for 24 hours. The film was taken and washed with MEM without serum. 3-(4,5-Dimethyl-2-thiazolyl)-2,5-diphenyl-tetrazolium bromide (MTT) was added and again incubated for 4 hours to determine cell viability [21]. The % cell viability was calculated using the following formula:

$$\% \text{ Cell viability} = (\text{Optical density of treated cells/optical density of sample}) \times 100$$

Equipment

The functional groups present in the polyesters can be identified with KBr using a Perkin Elmer IR Spectrometer. The ^{1}H NMR Spectra of pre-polyesters can be determined by dissolving in d_6-DMSO solvent using AV 3500 MHz spectrometer. MALDI-MASS analysis was carried out by using Bruker Daltonics instrument. Dihydroxy benzoic acid was used as matrix and NaI was used as ionizing agent. The DSC studies were recorded at a heating rate of 10 ºC/min using a Perkin-Elmer Pyris I analyser. A Siemens D 500 Diffractometer with CuKα, Ni filtered radiation was used for assessing crystallinity of polymers. The sample is continuously scanned over the 2θ range from 5º to 80º and were utilized for quantitative phase analysis. Mechanical studies were carried out using Hounsfield instrument with 50 kilo newtons. The mechanical properties of polyesters and its composite thin films were measured and their values were calculated. The structure and morphology of polyester (PHSeC) and nanocomposite thin films were studied using a HITACHI S-3000 scanning electron microscope (SEM). Transmission electron microscope (TEM) (HR-TEM, Model-HITACHI, and H-7650) was used to analyze the surface morphology and the nanocrystalline size of nano-HAp powders. In order to prepare sample for TEM analysis, nano-HAp powders were dispersed evenly in ultrasonicator using methanol and poured a drop on carbon support film [22].

RESULTS AND DISCUSSION

Fourier-transform infrared (FT-IR) spectroscopy

In Figure 1, the symmetric stretching vibration at 1050 cm^{-1} depicts the presence of phosphate ion group in HAp. A broad band appears between 3350 cm^{-1} and 3550 cm^{-1} is due to –OH group. A peak at 1632 cm^{-1} is due to water molecules. Peaks around 1457 cm^{-1} shows the presence of carbonate ion in HAp.

The infrared spectra of synthesized polyesters PHSeC and its nanocomposite is shown in the Figure 2(a and b), respectively. In Figure 2(a) the presence of carbonyl group present in the ester can be confirmed by the peaks appeared at 1720 cm^{-1}. The peaks appeared at 1176 cm^{-1} showed the presence of C-O-C stretching vibrations of ester groups. The peaks appeared at 2935 cm^{-1} was due to methylene ($-CH_2-$) groups from diacids or diols [23]. A broad peak appeared at 3469 cm^{-1} confirms the presence of hydrogen bonding in hydroxyl groups.

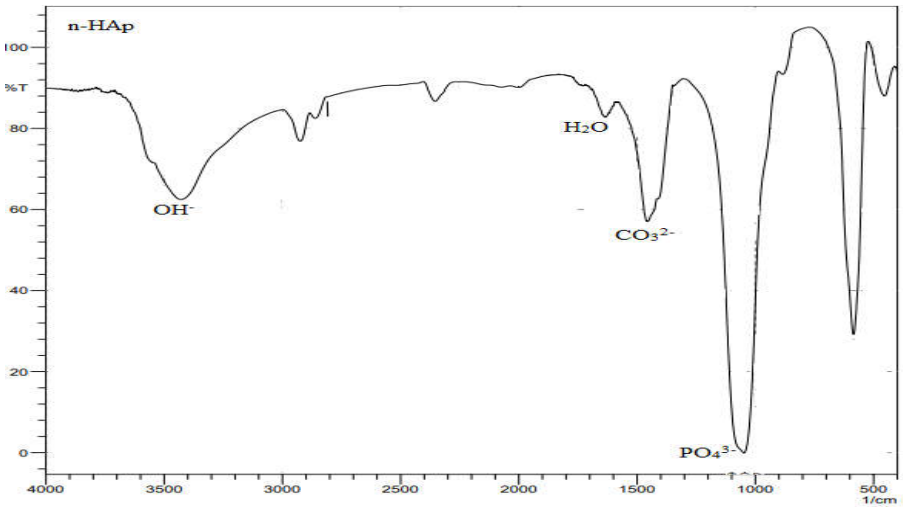

Figure 1. FT-IR spectrum of nano hydroxy apatite.

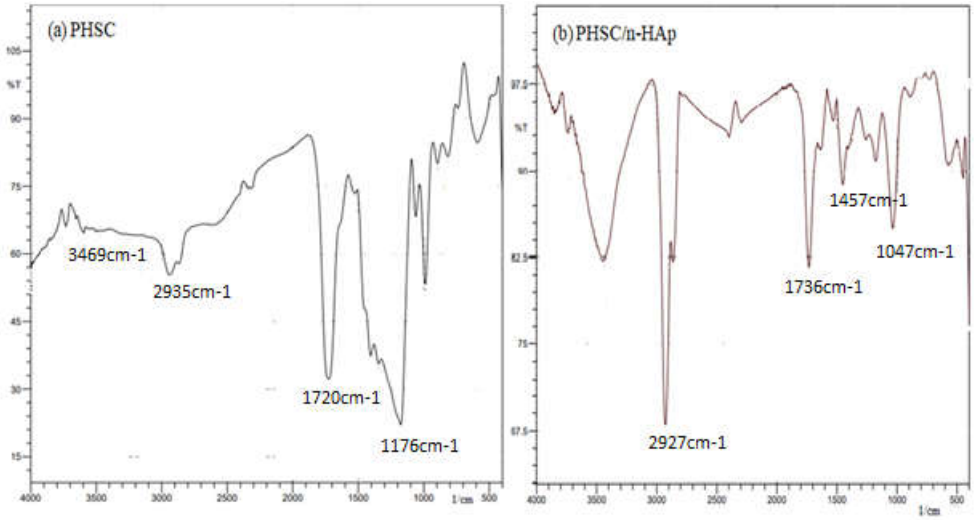

Figure 2. FT-IR spectra of (a) PHSeC and (b) nanocomposite.

Figure 2(b) shows that the pronounced peaks around 1047 cm^{-1} suggest the presence PO_4^{3-} group in polymer nanocomposites. Peaks at 1736 cm^{-1} shows the presence of carbonyl (C=O) groups from the ester group. This shows that composite contained both n-HAp and polyester functional groups. It can also be seen that -C=O bands around 1720 cm^{-1} are shifted to 1736 cm^{-1} This change in shift shows that there is weak interaction between ester carbonyl groups of polymers due to the presence of nano HAp in nanocomposites [24, 25]. It can be observed that PO_4^{3-} peaks of n-HAp at 1050 cm^{-1} shifted to little lower wavelength at 1047 cm^{-1} in the polymer composite. Such shifting may occur due to interactions between the PO_4^{3-} in nano HAp and the polymer in the composite [26].

^{1}H NMR spectra of polyester

In Figure 3, the various peaks appeared at 2.83 ppm were attributed to the methylene protons of citric acid. The multiple peaks located at 3.38 ppm were due to protons in $–OCH_2CH_2–$ group from HD [1]. The peaks appear at 1.53 ppm were due to central $–CH_2$ group of diacids. The multiple peaks located at 2.23 ppm were attributed to the protons in $–CH_2CO$ group.

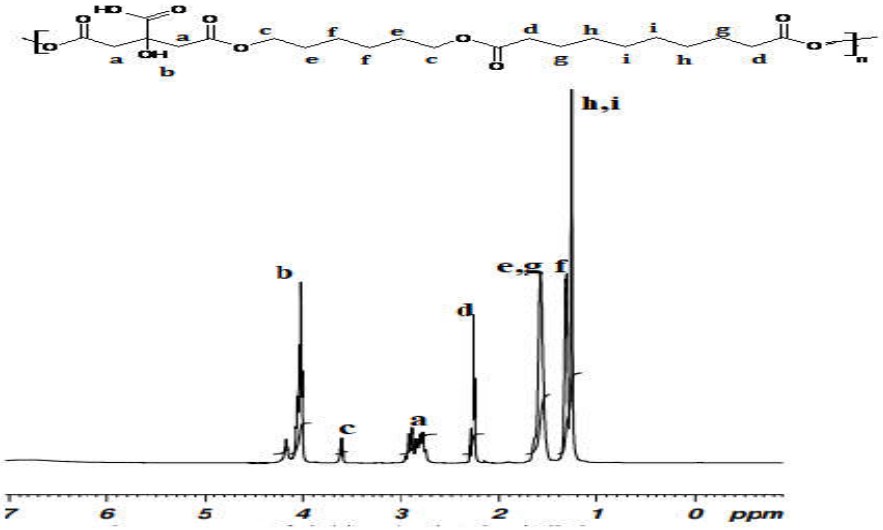

Figure 3. ^{1}H NMR spectrum of PHSeC.

Differential scanning calorimetry of polyesters

The DSC heating thermograms of PHSeC and the corresponding nanocomposite (15% n-HAp/polymer) are depicted in Figure 4. Usually, the composite is affected by the factor such as chemical cross-linking density. In the DSC thermogram, the reduction of Tg arises due to the incorporation of nano-HAp which hinders the further cross linking of polymers. The glass transition temperature (Tg) of polyester is around -32.3 ^oC and its nanocomposite is observed around -37.9 ^oC. This occurs due to the decrease in cross-linking density when n-HAp was incorporated into the PHSeC polymer.

XRD analysis of n-HAp

An X-ray diffractogram pattern of nano-HAp powder calcined at 500 ^oC is shown in the Figure 5. The XRD study indicated that the synthesized nanomaterial was crystalline structure. The appearance of sharp peaks confirms the formation of crystalline phase. There were no characteristic peaks of impurities which shows that prepared nano-HAp was of high purity. The XRD technique was carried out over the diffraction angle in between 2θ (10-80^o). The peaks of Figure 5 can be indexed as a hexagonal phase of hydroxyapatite with a lattice constant of a = 9.418 Å and c = 6.884 Å, in good agreement with JCPDS card no. 09-0432. In prepared hydroxyapatite, the peak at 31.8° corresponding to the plane (211). The peak position at 21.84, 22.98, 25.79, 28.07, 28.98, 34.12, 35.47, 39.86, 42.13, 43.80, 45.38, 46.72, 48.19, 49.48, 50.57, 52.08, 53.05, 55.98, 61.71, 64.09, 65.08, and 77.08 are in accordance to plane of (200), (111),

(002), (102), (210), (202), (301) (310), (311), (113), (203), (222), (312), (213), (321), (402), (004), (322), (214), (323), (511), and (513) with the hydroxypatite phase [27]. Some other phases could not be detected in the pattern. The Scherrer formula [28] is used to calculate the crystalline size of the nanoparticles:

$$d = \frac{0.94\lambda}{\beta \cos \theta}$$

where d is the diameter of the crystalline particle, λ is the wavelength of X-ray radiation, B is the full width at half-maximum (FWHM) of the peak and θ is the angle of diffraction. The crystalline size of the nanoparticle obtained is 28 nm.

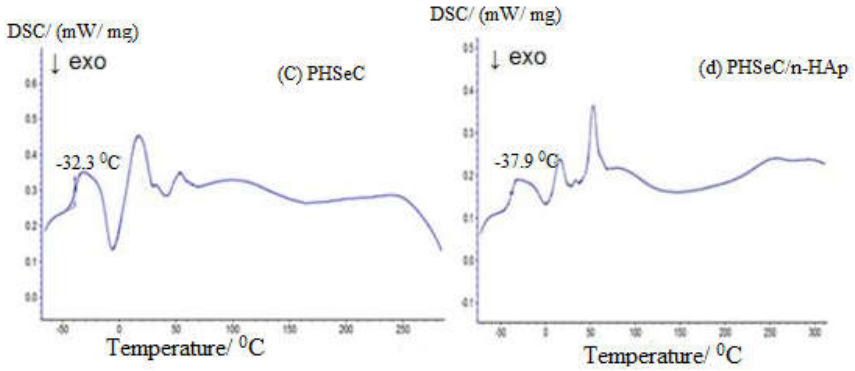

Figure 4. DSC thermogram of PHSeC and its nanocomposite.

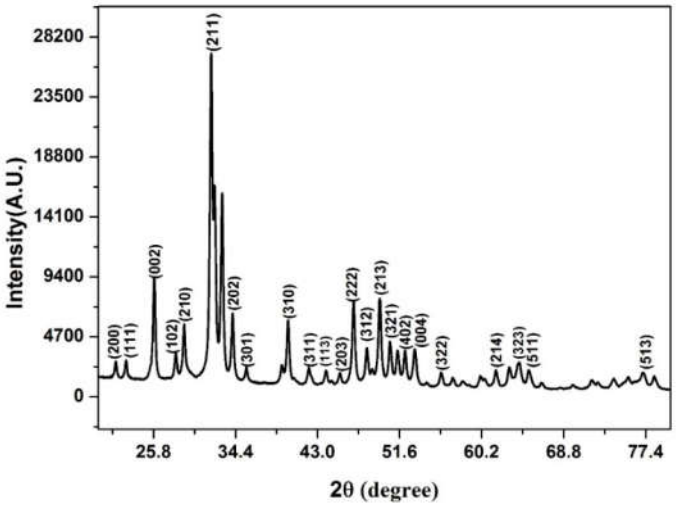

Figure 5. X-Ray diffractogram of n-HAp.

Mechanical properties

As shown in Table 1, it can be observed that after incorporating nano-HAp powders into polyester, the tensile strength, the modulus of composites and the elongation have been increased. Increase in mechanical properties occurs due to increased interaction between matrix and n-HAp. From the table, it is observed that the PHSeC polymer nanocomposite exhibits better modulus value. The properties of sebacate and citrate polyesters composites are comparable to natural extracellular matrix (ECM) components, which are soft and elastic polymer provides mechanical stability to living organisms [29, 30]. Therefore poly(1,6-hexanediol-sebacate-citrate) is used for further studies such as scaffold fabrication and cytotoxicity test. The high tensile strength is due to result of the interfacial interaction between the polyester and nanocomposite surface.

Table 1. Mechanical properties of n-HAp/polymer composite.

Polymer	%n- Hap	Tensile strength (MPa)	Young's modulus (MPa)	Elongation at break (%)
PHSeC	0	0.140	0.931	14.64
	15	0.175	1.864	26.19

Transmission electron microscopy (TEM)

The morphological studies of the nano-hydroxyapatite, sintered at 500 °C were observed by the TEM, as shown in Figure 6. Agglomeration of nano-HAp particles was also observed. The transmission electron microscopic analysis confirms the presence of the spherical shape morphology of the prepared hydroxyapatite in the nanometer scale. The particle size has been enhanced by increasing temperature, which may be due to faster growth rate at higher temperatures [31]. At lower calcination temperature, there is possibility of reducing the particle size but with a poor mechanical property. At higher calcination temperature especially above 600 °C, the particle size of hydroxy apatite increases which becomes more brittle as it is not suitable for fabricating scaffolds. Hence, we chose 500 °C is the optimum temperature for preparing nano hydroxy apatite. The particle size increased to 30-70 nm. The TEM images in Figure 6 demonstrate that the n-HAp powders fabricated by sol-gel method used in this study were in the sub-micron to nano-size range with all having dimensions of 30-70 nm.

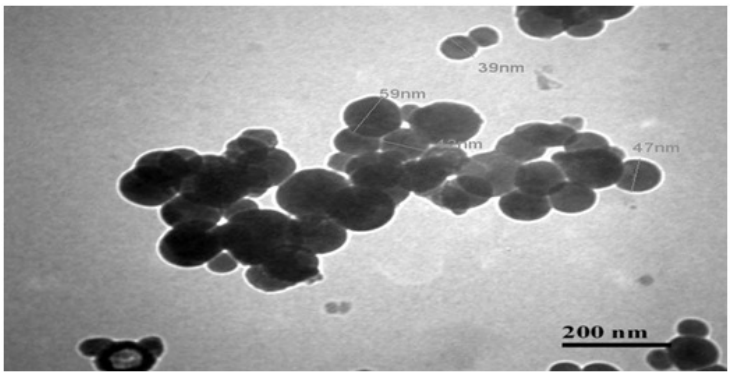

Figure 6. TEM images of n-HAp.

Scanning electron microscopy (SEM)

The SEM images demonstrated that many particles of different sizes were seen with small bright spots and fairly well spread across the image. The distribution of n-HAp particles in polymer was shown in the Figure 7 depicted that the composite was not agglomerated because of strong interfacial interaction between n-HAp and polymer matrix for the polymers filled with 15 wt% of n-HAp.

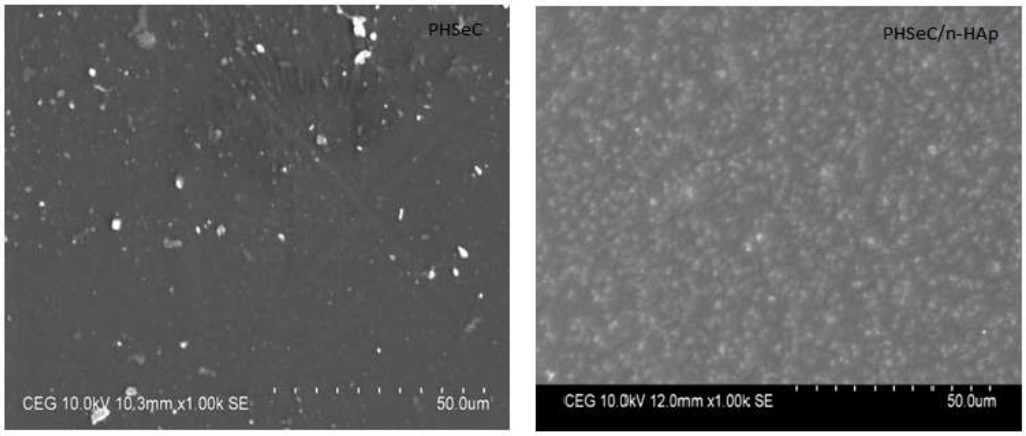

Figure 7. SEM photographs of PHSeC polyester thin film and PHSeC/n-HAp(15%) composite thin film

In vitro assay for cytotoxic activity (MTT assay)

When vero cells were incubated onto poly(1,6-hexane diol-ssebacate-citrate)/nanoHAp polymer nanocomposite thin film, the cell adhesion of polymer nanocomposite was observed for 24 h after cell seeding. Cell adhesion was quantitatively evaluated using MTT assay as shown in the Figure 8.

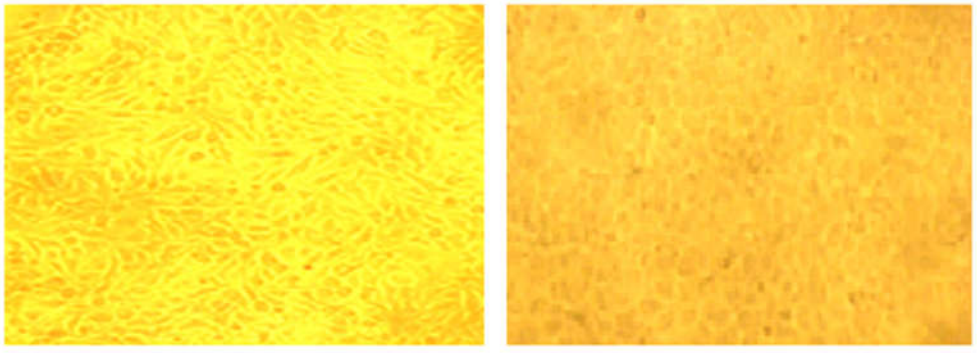

Normal vero cells Cell adhesion after 24 h on PHSeC/n-HAp

Figure 8. Photomicrograph of cell adhered to the surface of nanocomposite.

The O.D. value reflect directly the number of living cells [32]. The cells are fixed to the surface can be seen by photomicrograph taken. The photomicrograph showed that the density of cell lines increased on polymer nanocomposite thin film. The optical density (O.D.) values of control and nanocomposite obtained are 0.41 and 0.54, respectively. The results indicated that polymer nanocomposite showed a higher percentage of cell viability of 75.92%. These results demonstrate that polymer possesses significant cell viability. Surface modification with cell-adhesive collagen could further increase cell adhesion. It indicates that the polymer nanocomposites show better biocompatibility over cell growth.

Fabrication of porous scaffold of PHSeC nanocomposite

Figure 9(A and B) photographs of PHSeC nanocomposite scaffold images (C) SEM image of porous scaffold produced by particulate-leaching technique; (D) SEM image of porous scaffold with n-HAp size respectively (scale bar: 500 nm); and (E) SEM images of PHSeC–15%n-HAp surface within porous scaffold (scale bar: 500 nm)

In Figure 9 (A and B) the photographs of scaffold appear very elastic in nature which can be used in tissue engineering. The size of porosity in scaffold increased with the addition of n-HAp. HA nanoparticles are distributed and surrounded by the polymer as shown in the SEM Figure 9 (C and D) and the size of nanoparticle ranges between 30-70 nm.

Ali Moradi *et al.* [33] fabricated scaffold using citric acid and 1,8-octane diol along with micro hydroxyapatite. It is well known that poly(1,8-octanediol-co-citrate) (POC) has notable properties for scaffold fabrication and in tissue engineering. Rectangular pore shapes are appeared in scaffold. In this study, we have used monomers such as citric acid, sebacic acid and 1,6-hexane diol monomers for the synthesis of poly(1,6 hexanediol-sebacate-citrate), PHSeC. In SEM image of porous scaffold Figure 9(D), pentagonal pore shape appeared shows that the polymer nanocomposite has high stiffness due to increased mechanical strength in comparison to polymer composite as in POC/HA [33]. The size of pores in PHSeC/n-HAp are appeared in nano-size which facilitate the suitable material for tissue engineering.

Scanning electron microscopic investigations in Figure 9(E) revealed lumps-like structure with nanometer size in scaffold appeared consisting in polymer nanocomposite skeleton with pores throughout the scaffold.

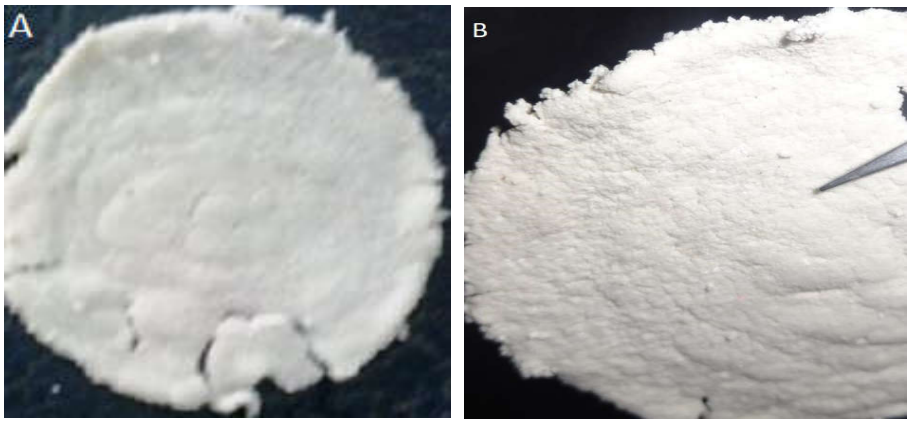

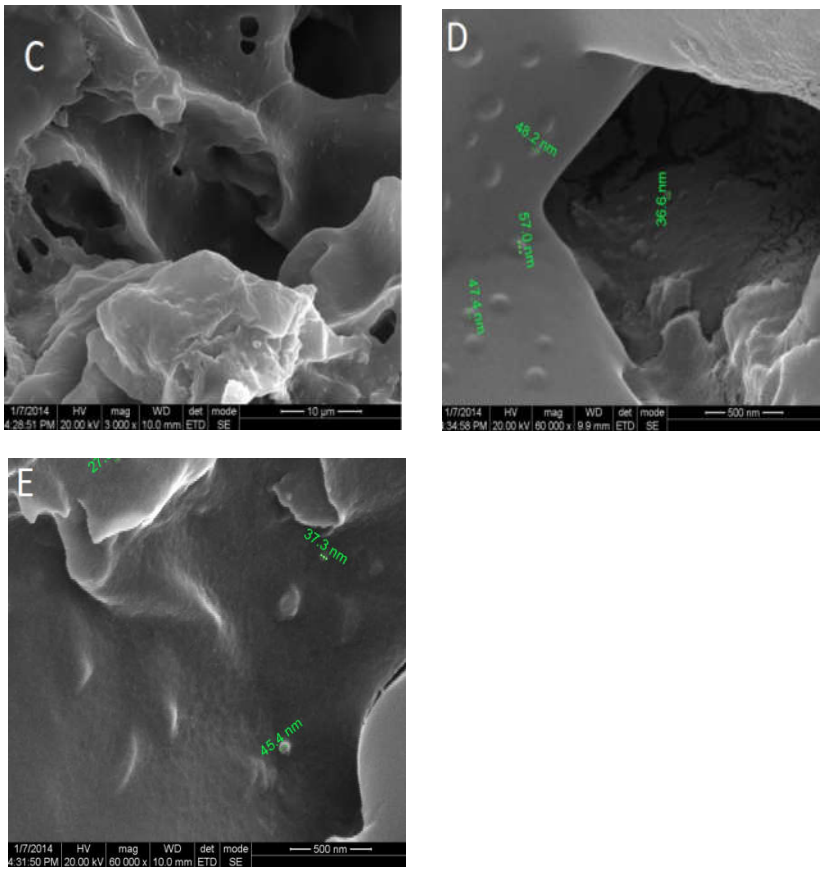

Figure 9. PHSeC nanocomposite scaffold images.

CONCLUSION

A novel polymer nano-composite scaffold material was fabricated in three steps: (i) polycondensation method with 1,6-hexanediol, sebacic acid and citric acid as monomers and without adding catalyst; (ii) preparing polymer nanocomposite using nano hydroxyapatite particles and (iii) further blending with porogen and subsequently removed the porogen by salt-leaching method. The prepared polymer composites are elastic in nature, which is proved from mechanical studies. The pore sizes in the scaffold are in nanometric scale and the nature of the polymer matrix and in the scaffold provides effective application in engineering of functional bone tissue for reconstructive surgery. Scanning electron microscopy analysis of the nano-hydroxy apatite, polyester, the nanocomposite and scaffold are carried out and morphologies are examined. The SEM image shows the agglomeration of nanosized grains of hydroxyapatite. The structure and morphology of nano hydroxy apatite were confirmed by transmission electron microscopy analysis of nano-HAp confirmed the spherical structure in the dimension of 30 to 70 nm. *In vitro* assay for Cytotoxicity activity (MTT assay) proved the polymer nano composite is biocompatible in nature.

REFERENCES

1. Yang, J.; Webb, A.R.; Pickerill, S.J.; Hageman, G.; Ameer, G.A. Synthesis and evaluation of poly (diol citrate) biodegradable elastomers. *Biomaterials* **2006**, 27, 1889-1898.
2. Gang, L.; Shuhao, Q.; Xiaonan, L.; Daohai, Z.; Min, H. Structure and properties of nano-hydroxyapatite/poly (butylene succinate) porous scaffold for bone tissue engineering prepared by using ethanol as porogen. *J. Biomater. Appl.* **2018**, 33, 776-791.
3. Ciobanu, C.S.; Popa, C.L.; Predoi, D. Cerium doped hydroxyapatite nanoparticles synthesized by coprecipitation. *J. Serb. Chem. Soc.* **2016**, 81, 433-446.
4. Ergun, C. Effect of Ti ion substitution on the structure of hydroxylapatite. *J. Eur. Ceram. Soc.* **2008**, 28, 2137-2149.
5. Sooboo, S.; Sreekanth, B.J. Synthesis of thermally stable metal substituted hydroxyl apatites for the selective oxidation of light paraffins. *Bull. Chem. Soc. Ethiop.* **2013**, 27, 57-68.
6. Saranya, K.; Meenal, K.; Sutapa. Synthesis of hydroxyapatite nano powders by sol–gel emulsion technique. *R.R. Bull. Mater. Sci.* **2011**, 34, 1749-1753.
7. Xiao, W.; Sonny, B.B.; Rahaman, M.N. Preparation of resorable carbonate-substituted hollow hydroxyapatite microspheres and their evaluation in osseous defects in vivo. *Mater. Sci. Eng. C. Mater. Bio. Appl.* **2016**, 60, 324-332.
8. Kundu, B.; Sinha, M.K.; Mitra, S.; Basu, D. Synthetic hydroxyapatite-based integrated orbital implants. *Indian J. Ophthalmol.* **2005**, 53, 235-241.
9. Yadesa, W.; Taddesse, A.M.; Kibret, K.; Dechassa, N. Synthesis and characterization of Fe-Al-Mn nanocomposite sorbent for phosphate sorption-desorption study. *Bull. Chem. Soc. Ethiop.* **2018**, 32, 421-436.
10. Scaglione, S.; Lazzarini, E.; Ilengo, C.; Quarto, R.A. Composite material model for improved bone formation. *J. Tissue Eng. Regener. Med.* **2010**, 4, 505-513.
11. Dhiraj, M.; Suja, G.; Poonam, M. Synthesis of hydroxyapatite by chemical precipitation technique and study of its biodegradability. *Int. J. Res. Adv. Technol*. **2014**, 2, 159-161.
12. Yushi, Y.; Qingzhi, W.; Min, W.; Jia, L.; Zhou, M. Xiaohui, C. Hydrothermal synthesis of hydroxyapatite with different morphologies: Influence of supersaturation of the reaction system. *Cryst. Growth Des.* **2014**, 14, 4864-4871.
13. Barakat, N.A.M.; Khil, M.S.; Omran, A.M.; Sheikh, F.A.; Kim, H.Y. Extraction of pure natural hydroxyapatite from the bovine bones bio waste by three different methods. *J. Mater. Process. Technol.* **2009**, 209, 3408-3415.
14. Sharifah, A.; Iis, S.; Mustapha, H. Mechanochemical synthesis of hydroxyapatite nanopowder: Effects of rotation speed and milling time on powder properties. *Appl. Mech. Mater.* **2012**, 110, 3639-3644.
15. Nahanmoghadam, A.; Asemani, M.; Goodarzi, V.; Barough, S.E. In vivo investigation of PCL/PHBV/Hydroxyapatite nanocomposite scaffold in regeneration of critical-sized bone defects. *Fibers Polym.* **2021**, 22, 2507-2516.
16. Liu, D.M.; Troczynski, T.; Tseng, W.J. Water-based sol-gel synthesis of hydroxyapaptite: Process development. *Biomaterials* **2002**, 23, 1227-1230.
17. Sanosh, K.P.; Chu, M.C.; Balakrishnan, A.; Kim, T.N.; Cho, S.J. Preparation and characterization of nano-hydroxyapatite powder using sol-gel technique. *Bull. Mater. Sci*. **2009**, 32, 465-470.
18. Agrawal, K.; Gurbhinder, S.; Puri, D.; Prakash, S. Synthesis and characterization of hydroxyapatite powder by sol-gel method for biomedical application. *J. Miner. Mater. Charact. Eng*. **2011**, 10, 727-734.
19. Lano, J.J.M.; Chung, E.J. Engineering citric acid-based porous scaffolds for bone regeneration. *Methods Mol. Biol.* **2018**, 1758, 1-10.
20. Djordjevic, I.; Choudhury, N.R.; Dutta, N.K. Kumar, S. Synthesis and characterization of novel citric acid-based polyester elastomers. *Polymer* **2009**, 50, 1682-1691.

21. Weijia, L.; Jing, Z. Yuyin, X. Study of the in vitro cytotoxicity testing of medical devices (review). *Biomed. Rep.* **2015**, 3, 617-620.
22. Bilton, M.; Brown, A.P.; Milne, S.J. Sol-gel synthesis and characterization of nano-scale hydroxyapatite. *J. Phys. Conf. Ser.* **2010**, 241, 012052.
23. Kaihara, S.; Matsumura, S.; Fisher, J.P. Synthesis and characterization of cyclic acetal based degradable hydrogels. *Eur. J. Pharm. Biopharm.* **2008**, 68, 67-73.
24. Brioude, M.M.; Guimaraes, D.H.; Fiuza, R.D.D.; Prado, L.A.S.; Boaventura, J.S.; Nadia, J.S.; Josea, N.M. Synthesis and characterization of aliphatic polyesters from glycerol, by-product of biodiesel production, and adipic acid. *Mater. Res.* **2007**, 10, 335.
25. Nejati, E.; Firouzdor, V.; Eslaminejad, M.B.; Bagheri, F. Needle-like nano hydroxyapatite/poly(L-lactide acid) composite scaffold for bone tissue engineering application. *Mater. Sci. Eng., C.* **2009**, 29, 942-949.
26. Kang, Y.; Yang, J.; Khan, S.; Anissian, L.; Ameer, G.A. A new biodegradable polyester elastomer for cartilage tissue engineering. *J. Biomed. Mater. Res. Part A.* **2006**, 77A, 331-339.
27. Gallinetti S.; Cristina, C.; Ginebar, M.P.; Ferreria, J. Development and characterization of biphasic hydroxyapatite/ β-TCP cements. *J. Am. Ceram. Soc*. **2014**, 97, 1065-1073.
28. Hassan Farooq, M.; Aslam, I.; Sadia Anam, H.; Tanveer, M.; Rizwan, M. Defect engineering for improved photocatalytic performance of reduced lead titanate ($PbTiO_3$) under solar light irradiation. *Bull. Chem. Soc. Ethiop.* **2019**, 33, 373-380.
29. Webb, A.R.; Yang, J.; Ameer, G.A. Biodegradable polyester elastomers in tissue engineering. *Expert Opin. Biol. Ther.* **2004**, 4, 801-812.
30. Weng, H.T.; Mat, U.W.; Mohammed, R.A.K.; Tuck, W.W.; Onn, H. Polyol based biodegradable polyesters: A short review. *Rev. Chem. Eng.* **2015**, 32, 201-221.
31. Yusriha, M.Y.; Midhat, N.A.S.; Adilah, A. Preparation of hydroxyapatite nanoparticles by sol-gel method with optimum processing parameters. *American Institute of Physics* **2015**, 1660, 070054.
32. Liu, Q.; Wu, J.; Tan, T.; Zhang, L.; Chen, D.; Tian, W. Preparation, properties and cytotoxicity evaluation of a biodegradable polyester elastomer composite. *Polym. Degrad. Stab.* **2009**, 94, 1427-1435.
33. Moradi, A.; Dalilottojari, A.; Murphy, B.P.; Djordjevic, I. Fabrication and characterization of elastomeric scaffolds comprised of a citric acid-based polyester/hydroxyapatite microcomposite. *Mater. Design*. **2013**, 50, 446-450.